Atmospheric boundary-layer across Hadley and Ferrel cells over the Indian Ocean

G. S. Bhat*, Prashanth L. Rao and V. G. Sangolli

Centre for Atmospheric and Oceanic Sciences, Indian Institute of Science, Bangalore 560 012, India

A Southern Ocean Pilot cruise covering the latitudes from 10°N to 56°S in the open Indian Ocean was carried out during January–February 2004. Surface and upper air data collected during this cruise are reported here. It is shown that the broad features of the atmosphere, in particular that of temperature, follow the tropical and mid-latitude weather expected during January–February in this region. However, the atmospheric boundary-layer shows large variations, both in its height and structure between tropics and high latitudes. Strong influence of the surface heat flux on boundary layer structure is clearly seen. Humidity field reveals several local maxima and minima, suggesting a laminated atmosphere with air from different sources moving almost unmixed in adjacent layers.

Keywords: Atmospheric boundary-layer, Ferrel cell, Hadley cell, humidity, Indian Ocean, SST.

Introduction

THERE have been scientific expeditions in the Indian Ocean in the past in connection with the summer monsoon experiments (e.g. IIOE[1], MONEX-79 (refs 2, 3), BOBMEX[4], ARMEX[5]) and the Indian Ocean Experiment[6] (INDOEX) during the boreal winter. All these cruises, when considered together, covered the Indian Ocean north of 20°S, i.e. the tropical Indian Ocean. The Southern Ocean has been data sparse[7]. The Southern Ocean Pilot[8] (SOP) cruise offered an opportunity to make measurements from 10°N to 55°S in the open Indian Ocean during January–February. From the atmospheric point of view, this area is of interest in several respects. The cruise cut across Hadley and Ferrel cells[9] (Figure 1) encountering distinctly different weather systems, including the tropical convergence zone between equator and 20°S (during January–February) and subsidence dominated subtropical high. The sea surface temperature (SST) also shows a large variation with warm waters in the tropics, strong SST gradients between 40° and 50°S, and cold waters further south (Figure 2).

Thus, there is a large variation in the surface and upper air conditions and major changes in the surface fluxes are expected as well. The atmospheric boundary-layer (ABL),

which is the lowest part of the atmosphere constantly in touch with the underlying surface and responds to changes in the surface conditions on time scales of a few hours, could show large variation in its structure across these latitudes[10]. No previous measurement of ABL structure exists to the south of 20°S over the Indian Ocean, and how the boundary layer adjusts to varying surface conditions in the Indian Ocean is yet to be understood. Therefore, measuring surface meteorological variables and the
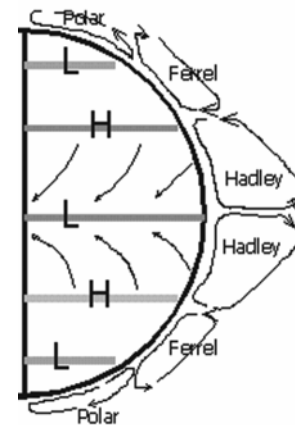

Figure 1. A schematic of atmospheric circulation cells in the meridional (north–south) direction[9]. H denotes surface pressure highs and the arrows within the semicircle indicate the direction of air motion near the surface. The cells outside the semicircle show the corresponding vertical circulation. Note that the rising and sinking regions associated with each cell move with the season.
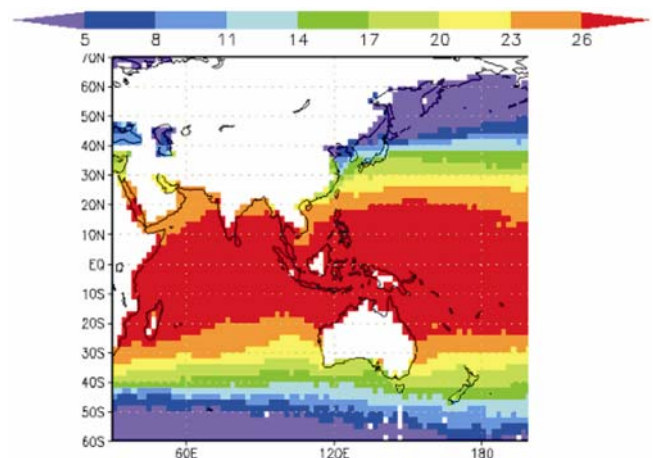

Figure 2. January climatological SST distribution[20]. The colour bar at the top shows the temperature values in degree Celsius.

*For correspondence. (e-mail: bhat@caos.iisc.ernet.in)

vertical thermal structure of the atmosphere during SOP offered to provide some initial data on the conditions of the atmosphere and ABL characteristics in this data-sparse region. The measurements were made from the Indian research ship *ORV Sagar Kanya* during January–February 2004. This study reports the surface conditions, ABL structure and upper air thermal structure observed during the SOP cruise. The results show that there is a large variation in ABL characteristics between Hadley cell and Ferrel cell latitudes. It is observed that the direction of heat transfer plays a critical role in determining the structure of ABL.

Experimental set-up

The experimental arrangement consisted of instrumentation for near surface and upper air measurements, and very similar to that installed by the Indian Institute of Science group during ARMEX[11]. An automatic weather system (AWS) was installed in an open area on the fore-castle deck of the ship. Wind speed (ff) and wind direction, air temperature (T_a) and relative humidity (RH), incoming solar and longwave radiation instruments were mounted on masts at a mean height of 11.5 m above sea level. Surface pressure (p_s) sensor was kept in the met lab where a Campbell CR10X data logger measured and archived data from all sensors. Data was sampled at 5 s interval, 5 min averages calculated and stored in the data-logger memory. Ship navigation data (course, heading and ship speed), needed to calculate the true wind speed and wind direction, was independently measured and archived. High resolution Vaisala radiosondes (model RS80-15G) were launched from the ship. It was planned to launch a radiosonde every 2.5° latitude interval to get a good north–south section of the atmosphere. Thus, the radiosonde launch time was not synchronized with synoptic hours.

Surface conditions

The latitudinal position of the ship during the onward journey as a function of time is shown in Figure 3 *a*. Figure 3 *b* shows radiosonde launch positions. Ship reached up to 56°S in the southern Indian Ocean. Except for a port call halt at Mauritius for a few days, ship was continuously moving with nearly constant velocity in the meridional direction (Figure 3 *a*). During the return cruise, a cyclone passed over the ship between 53°S and 54°S. Some sensors and AWS mast were damaged during the cyclone and AWS operation was called off during and after the cyclone. Therefore, observations made during the onward cruise are presented in the following.

Measured SST (Figure 4 *a*) is in good agreement with the January climatology shown in Figure 2. SST is more or less constant from 10°N up to 16°S with the warmest

water temperatures touching 30°C at 10°S. SST decreased gradually between 16°S and 27°S (change ~ 3°C), and then more rapidly between 28°S and 40°S. SST decreased by ~ 8°C over 2° latitude distance centred around 42°S. SST gradient is small southward of 43°S. Surface pressure is nearly featureless between 10°N and 25°S with only small amplitude variations around the mean (~ 1012 hPa) (Figure 4 *b*), and shows larger amplitude variations southward of 25°S that characterize mid latitude weather. The subtropical pressure high with p_s more than 1020 hPa was observed between 40°S and 44°S, i.e. around the latitudes of largest SST gradient.

Wind speeds were generally low to the north of 10°S (except around 4°N and over the equator) and more than 5 m s^{-1} between 10°S and 18°S (Figure 4 *c*). Winds change rapidly in the extra-tropics, and even over the subtropical high, wind speed was often high. RH shows large variations between 10°N and 20°S, with increase from 10°N to the equator, then fluctuating about a mean around 80–85% up to 20°S (Figure 4 *d*). RH decreased from values in excess of 90% at 30°S to less than 65% at 40°S. The equivalent potential temperature[12] (θ_e), a thermodynamic variable that depends on the temperature as well as the moisture content, is important in cloud formation and moist convective processes. θ_e was around 343 K at 10°N and increases to 350 K or more between 5°S and 20°S. These values are lower than those observed over the Bay of Bengal during the summer monsoon[13] and over the western Pacific warm pool[14], are nevertheless
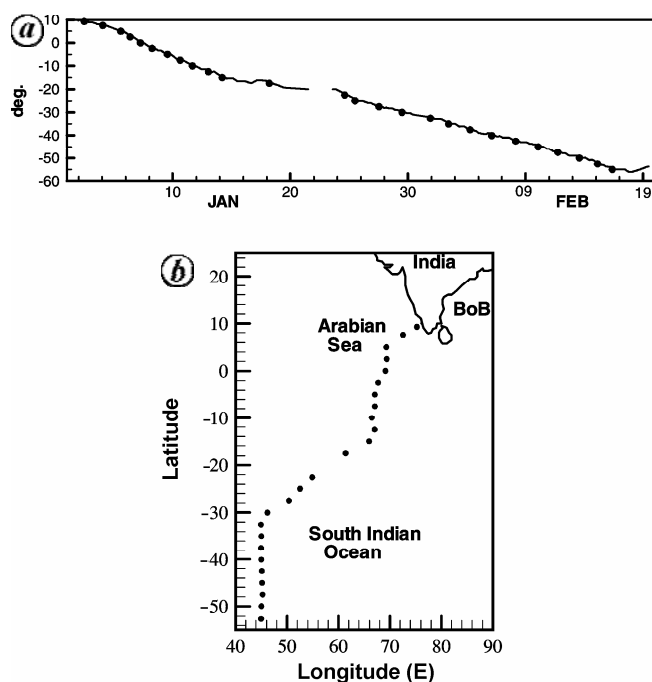

Figure 3. *a*, Change in the latitudinal position of *ORV Sagar Kanya* with time. Positive and negative values of latitude refer to north and south respectively. The filled circles show the time of radiosonde launch. *b*, Positions of radiosonde launch.
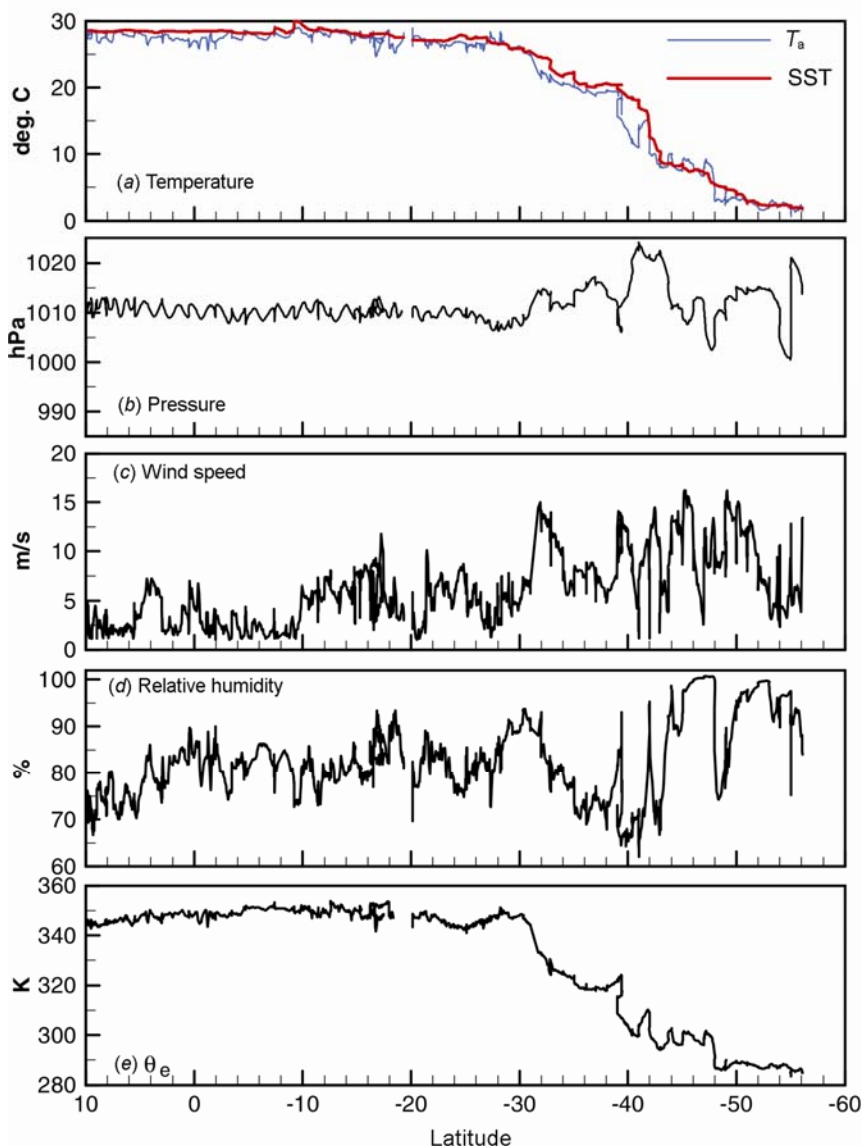
Figure 4. Latitudinal variation of surface variables. In obtaining this figure, 30 min average values are calculated first and plotted against the corresponding latitude.

sufficient to support deep convection in the tropics[15]. θ_e decreased between 30°S and 50°S with the most rapid decrease taking place between 30°S and 34°S. This is a combined effect of lower surface air temperature and lower RH.

The surface fluxes play an important role in determining the structure of ABL. Daily average fluxes of sensible heat (SH), latent heat (LH) and incoming global solar radiation (SW_{in}) are plotted against the corresponding latitude in Figure 5. Here, SW_{in} directed towards the surface and other fluxes directed away from the surface are taken positive. SW_{in} is high up to 36°S. Clouds strongly modulate SW_{in}, and observed variations appear to be more due to clouds. LH flux is less than 100 W m^{-2} north of 10°S and increases to 100 W m^{-2} or more between 11°S and 18°S, and the largest values (~ 300 W m^{-2}) are observed at

40°S. Southward of 44°S, LH fluxes are small and become comparable to SH fluxes. In fact, SH flux is small compared to SW_{in} and LH fluxes and its maximum value of 100 W m^{-2} occurs at 40°S. The small value of SH from 10°N to 30°S is owing to the difference between air temperature and SST being small in this area (Figure 4). Between 44°S and 48°S, SH flux is negative, i.e. ocean is gaining heat from the air above.

Vertical structure

Atmospheric boundary-layer

Air in ABL continuously interacts with the underlying surface, and surface conditions and fluxes strongly influ-

ence the ABL structure. Typically, ABL has a layer immediately above the surface where properties change rapidly with height (surface layer, SL). There is also a very thin interface layer where molecular diffusion processes dominate, however it is not possible to observe this in the radiosonde profiles because the starting point of radiosonde measurements is several metres above the surface. A layer, which is neutrally stable and known as mixed layer (ML), exists above SL[10]. Sometime, an inversion (a thin but very stable layer) caps ML while in other cases, there is no inversion as such but a stable layer overlies ML. Thermals that originate in the SL penetrate above ML, and this part of the atmosphere is also included in ABL[10]. However, with the radiosonde data alone, it is not possible to determine the upper reach of the thermals; in the following ABL top is taken to be the ML top. The virtual potential temperature (θ_v) is often used to characterize ABL[10]. (θ_v is the temperature that will result if air is compressed or expanded adiabatically to 1000 hPa. A correction for density change due to water vapour is included in the temperature term, hence the name virtual temperature[12].) A constant value of θ_v implies neutral stability whereas decreasing and increasing values with height imply unstable and stable stratification respectively[12].

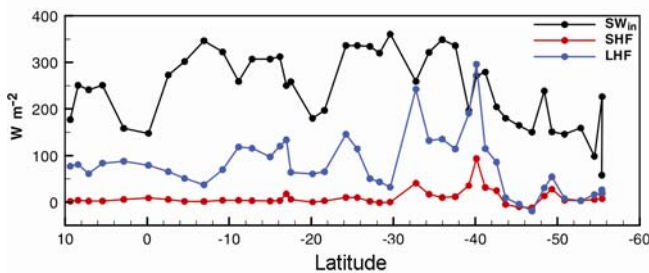**Figure 5.** Variations of daily average values of SW_{in}, sensible heat flux (SHF) and latent heat flux (LHF) with latitude.
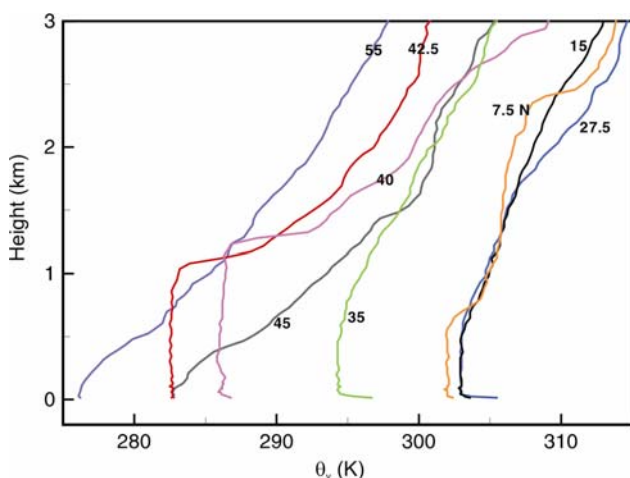

Figure 6. Vertical variation of θ_v in the lowest 3 km layer of the atmosphere showing ABL structure. The numbers on the lines refer to the latitude (south) and 7.5 N refers to 7.5°N.

Representative vertical profiles of θ_v at different latitudes are shown in Figure 6. At 7.5°N, ML top is around 550 m with a shallow SL and capped by an inversion. This structure is typical of tropics dominated by large scale subsidence[16,17]. The sounding at 15°S is typical of a convective atmosphere in the tropics with a ML that is 500–600 m deep, topped by a stable layer but without an inversion[17]. Similar profiles are observed over the head Bay during the summer monsoon[18]. The sounding at 27.5°S is very similar to that at 15°S in the lowest 1.5 km layer. The profile at 35°S is similar to that at 15°S except that it is shifted to the left as if the atmosphere cooled by about 9°C throughout. Thus, the height of ABL between 7.5°N and 35°S is in the 500–600 m range, which is normal in the tropical atmosphere[16,17]. The ABL structure changes dramatically between 35°S and 40°S, with ML much deeper and capped by a strong inversion in the latter position. Measured SH flux during the cruise is the highest at 40°S (Figure 5) and at the time of radiosonde launch, the surface wind speed is 13 m s⁻¹. Strong surface heating and high winds together produce a deep ABL. At 42.5°S (region of strongest SST gradient), ABL resembles that at 40°S except that its height is marginally less and there is no unstable layer near the surface. SH flux is very small at this location, and the boundary layer is wind-driven (wind speed was ∼ 8 m s⁻¹). At 45°S, ML is very shallow (< 100 m deep) and θ_v increases continuously with height. Here the surface winds are strong (∼ 12 m s⁻¹), but air is warmer than the water below (Figure 4 a) and SH flux was downward (Figure 5). Thus, despite strong winds, ML is very shallow. At 55°S, θ_v continuously increases with height and there is no ML. Here the SH flux is downward and winds are weaker (4.4 m s⁻¹). Thus, when the heat flux is downwards (i.e. underlying surface colder than the air above), ML collapses even if the winds are strong. Here the atmosphere is stable. It is possible to check if the Richardson number is above the critical value for instability[19] provided the wind data profile is also available. The radiosonde system used here has GPS wind finding capability, however, for reasons not clear, wind data is missing in the radiosonde profiles in high latitudes below 500 m. Therefore, this could not be tested.

Vertical thermal structure

Vertical profiles of temperature at selected latitudes are shown in Figure 7. Some of the low level inversions (layer where temperature increases with height) discussed above are clearly found in the temperature profiles. There are other inversions between 2 and 5 km. Although the temperature profiles at 35°S and 40°S look different below 2 km, they behave in a similar way above 3 km. Examination of temperature profiles reveals that at heights above 5 km, profiles between 10°N and 30°S, 32.5°S and 40°S, and southward of 42°S bunch together.
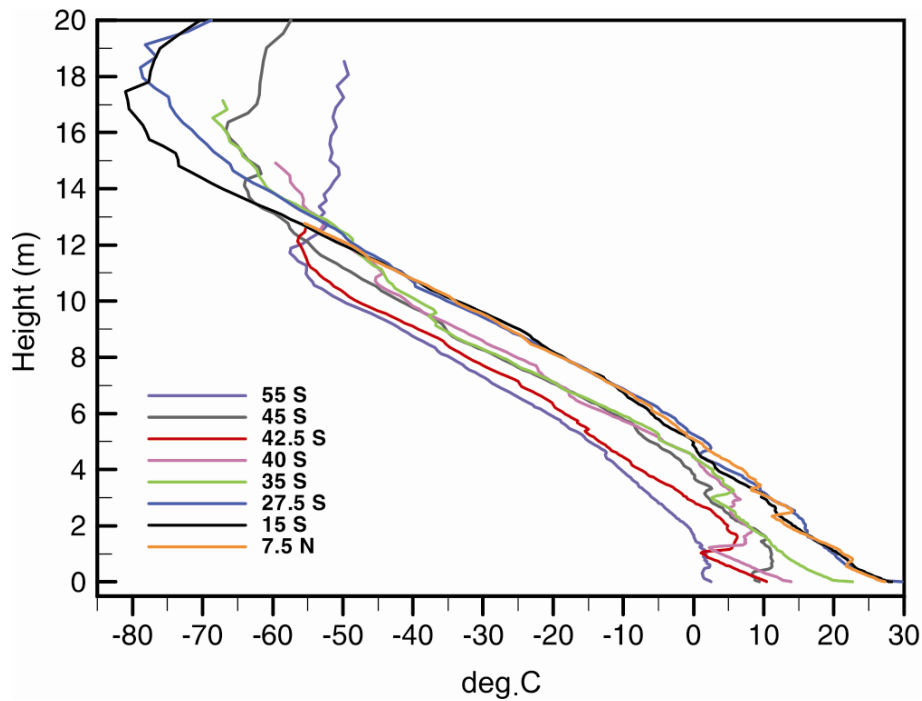
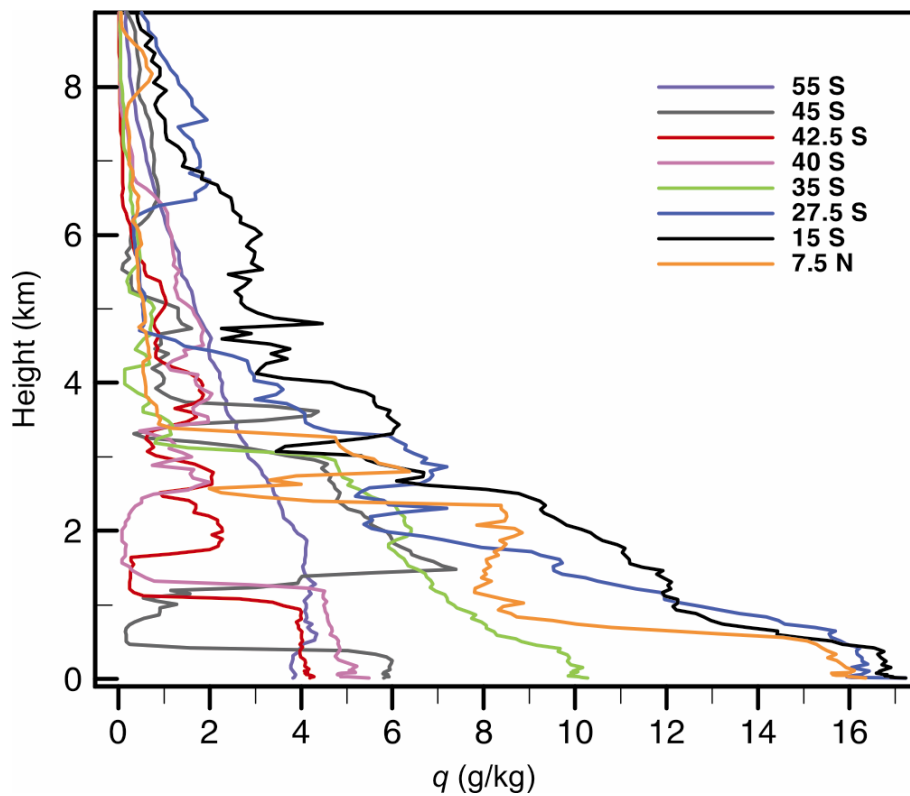**Figure 7.** Vertical variation of temperature at different latitudes.

Figure 8. Vertical variation of specific humidity (*q*) at different latitudes.

For the tropical soundings, the tropopause is between 17 and 18 km and coldest temperatures are found here. During January, the tropical convergence zone is in the latitude belt 5°–15°S, and the tropopause was expected to be deepest here, however, the tropopause was deepest at 27.5°S. Tropopause height decreases to 11.5 km at 55°S.

Vertical variation in specific humidity (the amount of water vapour per unit mass of air, q) is shown in Figure 8. The profiles of specific humidity vary a lot. In ML also, q generally decreases with height, and in the stable layer above ML, the decrease is pronounced in a majority of the profiles. There are regions with local maxima and minima, suggesting a laminated vertical structure with air from different sources moving in adjacent layers. Of particular interest is the profile at 45°S. Here, q is constant in the shallow ML, almost devoid of moisture between 500 and 750 m, and then with a very moist layer above 1.3 km.

Conclusions

The atmospheric data was collected successfully during the onward SOP cruise. The following are the main conclusions:

(i) Near the surface, measurements are consistent with what was expected based on climatology, namely, small or weak gradient in the tropics (up to 30°S), a large SST gradient between 40°S and 44°S, and cold water with smaller SST gradient further south.

(ii) The ABL structure responded to surface heat fluxes dramatically. When the heat flux was upwards, the ABL structure was similar to the standard one with a well defined SL and ML. However, when the heat flux was downwards, the SL became stable and ML collapsed even at wind speeds of more than 10 m s^{-1}.

(iii) Temperature profiles are along the expected lines with the exception that the highest tropopause height was observed at 27.5°S and not in the climatological position of tropical convergence zone (5°S–20°S during January).

(iv) Humidity profiles show complex structures, and suggest that air from different sources could be moving in thin layers one over the other unmixed.

1. Rao, T. S. S. and Griffiths, R. C., *Understanding the Indian Ocean: Perspectives on Oceanography* (IOC Ocean Forum II), UNESCO, Paris, France, 1988, p. 187.
2. Fein, J. S. and Kuettner, J. P., Report on the summer MONEX field phase. *Bull. Am. Meteorol. Soc*., 1980, **61**, 461–474.
3. Krishnamurti, T. N., Summer monsoon experiment – a review. *Mon. Weather Rev*., 1985, **113**, 1590–1626.
4. Bhat, G. S. *et al.*, BOBMEX – the Bay of Bengal Monsoon Experiment. *Bull. Am. Meteorol. Soc*., 2001, **82**, 2217–2243.
5. Rao, P. S., Arabian Sea Monsoon Experiment: an overview. *Mausam*, 2005, **56**, 1–6.
6. Mitra, A. P., INDOEX (India): introductory note. *Curr. Sci.*, 1999, **76**, 886–889.
7. King, J. C. and Turner, J., *Antarctic Meteorology and Climatology*, Cambridge University Press, 1988.
8. Pandey, P. C., Khare, N. and Sudhakar, M., Oceanographic research: Indian efforts and preliminary results from the Southern Ocean. *Curr. Sci.*, 2006, **90**, 978–984.
9. Lorenz, E. N., The nature and theory of the general circulation of the atmosphere. WMO monograph 218, World Meteorological Organization, Geneva, 1967.
10. Stull, R. B., *An Introduction to Boundary Layer Meteorology*, Kluwer, Dordrecht, 1988, p. 670.
11. Bhat, G. S., The Indian drought of 2002 – a sub-seasonal phenomenon? *QJRMS*, 2006, **132**, 2583–2602.
12. Emanuel, K. A., *Atmospheric Convection*, Oxford University Press, Oxford, 1994.
13. Bhat, G. S., Near surface variations and surface fluxes over the North Bay of Bengal during the 1999 Indian Summer Monsoon. *J. Geophys. Res.*, [*Atmos.*], 2002, **107**, 4336.
14. Kingsmill, D. E. and Houze Jr, R. A., Thermodynamic characteristics of air flowing into and out of precipitating convection over the west Pacific warm pool. *QJRMS*, 1999, **125**, 1209–1229.
15. Betts, A. K. and Ridgway, W., Coupling of the radiative, convective and surface fluxes over the equatorial Pacific. *J. Atmos. Sci*., 1988, **45**, 522–536.
16. Fitzjarrald, D. R. and Garstang, M., Vertical structure of the tropical boundary layer. *Mon. Weather Rev*., 1981, **109**, 1512–1526.
17. Lucas, C. and Zipser, E. J., Environmental variability during TOGA COARE. *J. Atmos. Sci.*, 2000, **57**, 2333–2350.
18. Bhat, G. S., Chakraborthy, A., Nanjundaiah, R. S. and Srinivasan, J., Vertical thermal structure of the atmosphere during active and weak phases of convection over the north Bay of Bengal: Observation and model results. *Curr. Sci.*, 2002, **83**, 296–302.
19. Turner, J. S., *Buoyancy Effects in Fluids*, Cambridge University Press, Cambridge, 1973.
20. Reynolds, R. W., Rayner N. A., Smith, T. M., Stokes D. C. and Wang, W., An improved *in situ* and satellite SST analysis for climate. *J. Climate*, 2002, **15**, 1609–1625.